A model for the global structure of self-similar vortex sheet roll-up

Jérôme Hœpffner[1,2*] and Marco Fontelos[3†]
[1] *Sorbonne Universités, UPMC Univ Paris 06, UMR 7190, Institut Jean le Rond d'Alembert, F-75005, Paris, France* [2] *CNRS, UMR 7190, Institut Jean le Rond d'Alembert, F-75005, Paris, France* [3] *Instituto de Ciencias Matemàticas, (ICMAT, CSIC-UAM-UCM-UC3M), C/ Serrano 123, 28006 Madrid, Spain*
(Dated: December 30, 2013)

Most vortices are born from the roll-up of a shear layer. The roll-up is traditionally modeled as the self-similar winding of an infinite spiral connected to a thin shear layer: a vortex sheet. We demonstrate a composite vortex sheet-point vortex model to quantify the global structure of two archetypal cases of self-similar roll-up. These cases are Kaden's single spiral solution of the wing-tip vortex and Pullin's double spiral solution of the nonlinear impulse response of the Kelvin-Helmholtz instability. The model consists in replacing the spiral with a point vortex of equal vortical intensity and accounting for the mutual interaction of the point vortex and the untouched sheet. We show that the model itself has an attractive self-similar solution which compares well with numerical experiments.

I. INTRODUCTION

The life of most vortices starts with a shear layer. A shear layer is a thin sheet of vorticity for instance produced by the motion of a flap in a fluid, see for instance [24]. This vorticity is a 2D object: a distribution of vortical intensity in the plane normal to the flap. Because of the flow motion, this zone is elongated. Helmholtz (see [8]) has developed a useful idealization of this type of elongated zone of vorticity by assuming it has zero thickness yet finite intensity: a *vortex sheet*. By doing so, he replaced a planar distribution of velocity by a moving line: a 2D object into a 1D model. This is a way to simplify the mathematical manipulations by considering simply the deformation of a line on the plane. According to the law of vortical induction, every point of the vortex sheet induce a motion of the other points of the fluid and also of the sheet itself, this is the self-induction of the vortex sheet: it deforms and evolves under its own influence.

Helmholtz [8] showed that this object is unstable: "The stationary forms of the surfaces of division are distinguished, as experiment and theory alike indicate, by a remarkably high degree of alterability when subject to the least disturbance, so that they comport themselves in some degree like bodies in unstable equilibrium". We read a few lines below "Theory points out that, wherever an irregularity is formed on the surface of an otherwise stationary current, this must give rise to a progressive spiral unrolling of the corresponding part of the surface".

Instability is an inherent property of vortex sheets, and lead them to roll into spirals. Prandtl exhibited in [19] a family of self-similar spirals built out of vortex sheets. His mathematical description provides us with a useful archetype to grasp the process of rolling up. Prandtl's solution was extended to multi-branched spirals by [1], and these results were translated into the integro-differential formulation of the Birkhoff-Rott equation by [15].

Once the spiral is formed, viscosity smears the line distribution of vorticity and a vortex is born. We have first followed the transformation from a 2D shear layer to a 1D vortex sheet, and the spiral roll-up is the next transformation from the 1D line to the 0D point vortex. This new step of idealization brings us to the well-known potential flow solution of the point vortex, see for instance [3]. A family of vortices evolve in the plane by inducing each-other a rotating motion. The velocity field is additive and the evolution can be described by the theory of dynamic systems. Interesting collective motion of a family of vortices have been exhibited, like for instance the finite time collapse of a triad of vortices into a single point, see [23].

For the present article, we would like to focus onto an intermediate step of this scenario from a 2D mixing layer to a 0D point vortex, just at the time when the vortex sheet is in the process of rolling up. We would like to make available a simple tool to simplify and quantify the hybrid dynamics of the spiral that is rolling and the sheet that is being rolled-up. One celebrated example of the composite dynamics of the spiral and the sheet is Kaden's description

*Electronic address: jerome.hoepffner@upmc.fr; URL: http://www.ida.upmc.fr/~hoepffner
†Electronic address: marco.fontelos@uam.es; URL: http://www.uam.es/personal_pdi/ciencias/afontelo

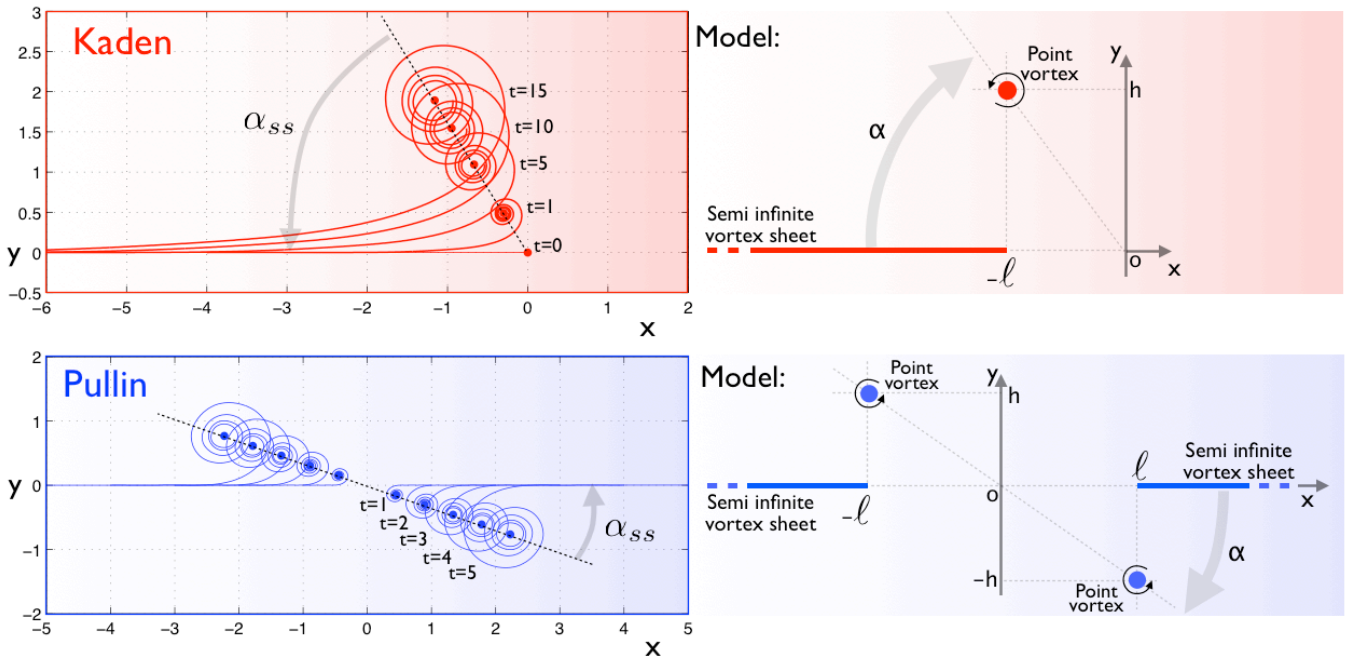

FIG. 1: Left: The evolution in time of the self-similar solutions of the infinitely thin shear layer for the Kaden (wing-tip vortex) and Pullin (Nonlinear impulse response of the Kelvin-Helmholtz instability). The self-similar angle is denoted α_{ss}. Data is digitized from [20] and [21]. Right: The structure of our models using semi-infinite vortex sheets and point vortices.

of the roll-up of a semi-infinite vortex sheet [14]. This flow evolution is akin to the formation of wing-tip vortices in the wake of airplanes, see [5]. The evolution of this flow is shown in figure 1, where data from numerical simulations is digitized from [20, 21]. The evolution of this vortex sheet is self-similar: it evolves in time without changing its shape. For instance, the center of the spiral moves along an oblique line with speed $Ct^{2/3}$. The exponent 2/3 dependency on time can be guessed from dimensional analysis and the fact that it translates along an oblique line is a direct consequence of self-similarity: geometrical proportions are conserved through the motion. Kaden has described in details the inner properties of the spiral. Here on the other hand, we would like to be in command of a conceptually and technically simple tool that can tell us the global structure of this flow: what is the value of the angle α between the spiral core's trajectory and the sheet initial position, and what is the speed at which this translation happens (i.e. what is the value of the prefactor C).

[20] approached this problem using numerical simulations. The Birkhoff-Rott equation (see [23]) is a complex integro-differential equation that describes the self-induction of a vortex sheet. The variables can be transformed into the self-similar coordinates suggested by dimensional analysis. Stationary states of this transformed equation correspond to self-similar evolutions of the vortex sheet. Pullin solved this nonlinear equation using the Newton iterative method, and found numerically the angle $\alpha = 57.8°$ and the amplitude $C = 0.58$.

If we have a simple tool to describe the large scale structure of Kaden's flow, it is straightforward to apply this tool to another self-similar vortex sheet roll-up. This is the nonlinear impulse response of the Kelvin-Helmholtz instability. [21] showed this family of double spiral solution of the vortex sheet equations. It is shown on figure 1. This nonlinear impulse response was also described using simulations of the Navier–Stokes equations in [10] for two-phase flows. In [17] it was studied in the context of ocean gravity waves and in [11] for the application to the atomization of a liquid jet. For an initially flat infinite vortex sheet, dimensional analysis tells that a nonlinear global self-similar solution should grow algebraically in time, so that the vortex cores translate at constant speed along a line with an angle α with the initial position of the shear layer. Once again here, we would like to be able to say with a simple model what should the speed of this translation be and what is the value of the angle α.

Pullin in [21] used the same methodology as in its previous paper for this double-branch solution, and obtained $\alpha \approx 18°$ and $V \approx 0.5$ (data digitized from its figures, and assuming that the velocity jump through the sheet is 2).

We would like to get quantitative information about the geometrical conformation of the spiral-sheet evolution, but we should as well be able to now more about its dynamics, and especially its stability. A self-similar solution is a useful particular solution for the evolution of a nonlinear system, but it is useful mostly if it is attractive: an unstable self-similar solution is unlikely to be observed in natural systems which are inherently noisy. For a review of computation of the stability of self-similar solutions, see [7].

II. MATHEMATICAL TOOLS

We need here a few tools from vortex dynamics, for a more complete treatment, see [23]. We want to describe the evolution of a thin line of vorticity moving in the plane. The sheet position is described using the complex notation

$$z = x + iy = z(\Gamma, t).$$

Each material point z of the vortex sheet is indexed by the circulation Γ between itself and origo. For instance, for an infinite horizontal sheet along the x axis, with constant intensity (the initial condition of Pullin's similarity solution) we have, following the notations of [16, 20, 22]:

$$\Gamma = 2ax,$$

where a is a dimensional constant. The local vortical intensity of the sheet γ is the local increase rate of the circulation along the sheet

$$\gamma = \frac{d\Gamma}{dx},$$

which is for our example equal to $2a$.

The presence of vorticity along a line indexed by Γ induces a velocity field everywhere described by the law of velocity induction

$$\overline{w}(z_0) = \frac{1}{2i\pi} \int_\Gamma \frac{d\Gamma}{z_0 - z(\Gamma)},$$

where $w = u + iv$ is the complex notation for the velocity vector at position z_0, u and v are the horizontal and vertical components of the velocity, and the overbar $\bar{\cdot}$ denotes complex conjugate. The integration is performed in the complex plane along the vortex sheet. We see here that the choice of indexing points on the sheet using the circulation Γ yields a very simple expression for the velocity field.

From this last expression, we can also obtain the velocity induced at z_0 by a point vortex of circulation Γ located at z

$$\overline{w}(z_0) = \frac{1}{2i\pi} \frac{\Gamma}{z_0 - z}.$$

The Birkhoff-Rott equation describes how the sheet evolves under self-induction

$$\frac{\partial \overline{z}}{\partial t}(\Gamma) = \frac{1}{2i\pi} \fint_{\Gamma'} \frac{d\Gamma'}{z(\Gamma) - z(\Gamma')},$$

where the integral is the Cauchy principal value integral.

III. KADEN'S WING TIP VORTEX

In this section we demonstrate the model on the case of Kaden's self-similar flow. This case is simple since there is only one vortex. The configuration of the model is displayed in figure 1. The vortex sheet initially lies on the semi-infinite line $x =]-\infty, 0[, y = 0$. Its vortical intensity by unit of length is $\gamma = a|x|^{-1/2}$, decreases away from origo. It must be decreasing, since if it had a constant intensity, the induced vertical velocity would be infinite everywhere.

Our model is sketched in figure 2. The spiral with core located at $x = -\ell(t), y = h(t)$ is replaced by a point vortex (we use this sign convention to ensure that ℓ and h are positive). The intensity Γ_0 of this point vortex is given by the integral of vorticity contained initially in the vortex sheet on the section $x \in [-\ell, 0]$. Essentially, we consider that this portion of the vortex sheet has been incorporated into the point vortex. In fact for the particular case of the Kaden's spiral, the intensity of the vortex is immaterial to its motion, but this reasoning will be used later for Pullin's case.

The velocity field induced by the vortex sheet at $\Gamma \in [-\infty, \Gamma_0]$ is

$$\overline{w}(z) = \frac{1}{2i\pi} \int_{\Gamma_0}^{\infty} \frac{d\Gamma'}{z + \Gamma'^2/4a^2} = \frac{a}{2\pi z^{1/2}} \left[\log \frac{z^{1/2} - i\Gamma'/2a}{z^{1/2} + i\Gamma'/2a} \right]_{\Gamma_0}^{\infty} = \frac{a}{2\pi z^{1/2}} \left(-i\pi - \log \frac{z^{1/2} - il^{1/2}}{z^{1/2} + il^{1/2}} \right). \tag{1}$$

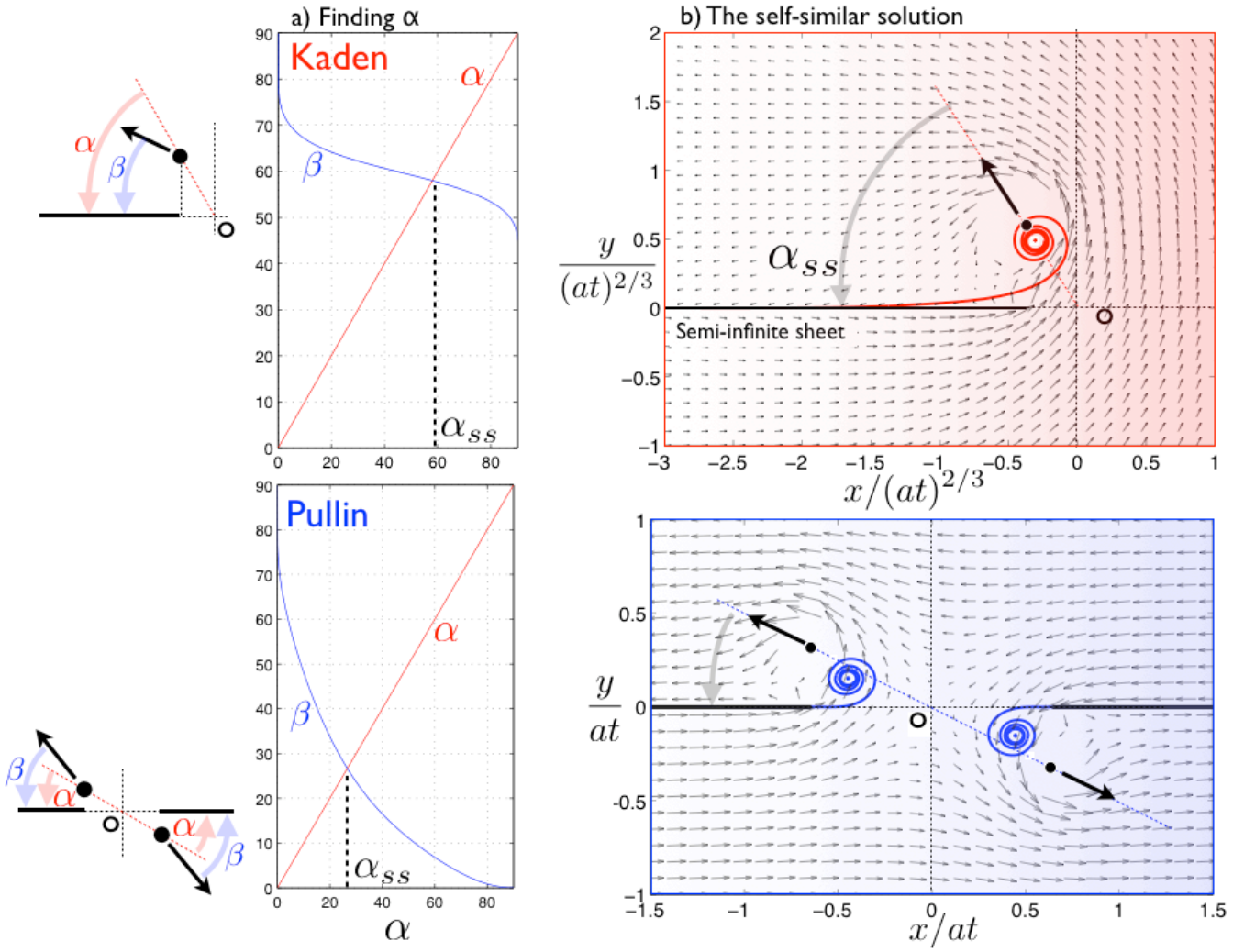

FIG. 2: The self-similar solutions for Kaden and Pullin. a) Finding the self-similar angle for the point vortex model, using (2) for Kaden and (4) for Pullin. This figure shows that the self-similar angle is stable. b) The position of the vortex centre in self-similar variables for the point-vortex model (black dot). The velocity field of the point vortex model is show. We compare to the self-similar solution of the Birkhof–Rott equations digitized from [20] and [21]

We seek the velocity at the position of the vortex core $z = -\ell + ih = \ell(-1 + i\tan\alpha)$

$$w(\ell,\alpha) = \frac{a}{\sqrt{\ell}}\frac{1}{2\pi(-1-i\tan\alpha)^{1/2}}\left(i\pi - \log\frac{(-1-i\tan\alpha)^{1/2}+i}{(-1-i\tan\alpha)^{1/2}-i}\right) = \frac{a}{\sqrt{\ell}}W(\alpha). \tag{2}$$

We see here that the velocity depends mainly on α, proportional to the sheet's intensity a and is lower when ℓ is larger: the systems slows down progressively as it grows in size.

There is a self similar evolution for a point vortex at z if there exist an angle α such that the velocity for this angle is aligned with Oz. Figure 2 shows that there exist a single solution. This corresponds to an angle $\alpha_{ss} = 57.98°$, remarkably close to the value 57.8° obtained in [20].

We see on the figure that the self-similar solution is stable: if the vortex is at a given time located above the self-similar trajectory ($\alpha > \alpha_{ss}$), we see that $\beta < \alpha$, thus the vortex is pushed down, and reciprocally, if the vortex is below the self-similar trajectory, ($\alpha > \alpha_{ss}$) then $\beta > \alpha$ thus the vortex is advected upward. The self-similar solution is thus globally attractive.

The angle is the first quantity that we can compare, but we can as well compare the velocity of the vortex compared to Pullin's solution. Supposing from initial time the vortex is located at this self-similar angle. Its induced velocity

is $u(\alpha_{ss})$. The vortex position evolves according to

$$\dot{\ell} = |w(\alpha_{ss})| \cos \alpha_{ss} = \frac{a}{\sqrt{\ell}} |W_{ss}| \cos \alpha_{ss},$$

which integrates into

$$\ell(t) = \left(\frac{3a}{2} |W_{ss}| \cos \alpha_{ss} t \right)^{2/3}.$$

We see appearing the 2/3 exponent of dimensional analysis. To compare with Pullin's numerical simulation we express this in the self similar reference frame

$$\xi_{ss} = \frac{\ell}{(at)^{2/3}} = \left(\frac{3}{2} |W_{ss}| \cos \alpha_{ss} \right)^{2/3} = 0.37, \quad \eta_{ss} = \xi_{ss} \tan \alpha_{ss} = 0.60.$$

This gives an amplitude prefactor for the velocity of $V = 0.70$. This is greater than Pullin's computed value of 0.58. This means that the point vortex model overpredicts the rate of growth of the self-similar structure.

This data is shown in figure 2 where we draw in self-similar coordinates the self-similar solution digitized from [20] and the location (ξ, η) of our point vortex using a black dot. We show as well the velocity field induced by the untouched vortex sheet and the point vortex from (1).

IV. PULLIN'S NONLINEAR IMPULSE RESPONSE

The velocity induced by a finite segment of vortex sheet of intensity a at $\Gamma \in [-\Gamma_0, \Gamma_0]$ with $\Gamma_0 = 2a\ell$ is

$$\overline{w}(z) = \frac{1}{2i\pi} \int_{-\Gamma_0}^{\Gamma_0} \frac{d\Gamma}{z + \Gamma/2a} = \frac{1}{2i\pi} \left[-2a \log \left(z - \frac{\Gamma}{2a} \right) \right]_{-\Gamma_0}^{\Gamma_0} = -\frac{a}{i\pi} \log \frac{z-\ell}{z+\ell}.$$

For an infinite sheet, the limit $\ell \to \infty$ applies. If the imaginary part of z is positive; the logarithm tends to $i\pi$ and if it is negative, it tends to $-i\pi$, thus the velocity is horizontal and equal to $-a$ above the vortex sheet, and a below the vortex sheet. The velocity jump across the sheet is thus $2a$.

The configuration of the model is displayed in figure 1. We need a formula for the velocity field induced by an infinite sheet whose central segment $x \in [-\ell, \ell]$ is removed

$$\overline{w}(z) = -a \, \mathrm{Sign}(\mathrm{Im}(z)) + \frac{a}{i\pi} \log \frac{z-\ell}{z+\ell}.$$

We assume the two point vortices symmetric with respect to O. Each vortex has circulation $\Gamma = 2a\ell$, equal to the circulation of a segment of length ℓ of the initial vortex sheet. The left hand side vortex is located at $z_l = -\ell + ih$, and the right hand side vortex is located at $z_r = \ell - ih$ (here once again, we use this sign convention to ensure that ℓ and h are positive). The velocity induced by the left vortex onto the right one is

$$\overline{w}_{lr}(z_r) = \frac{1}{2i\pi} \frac{2a\ell}{z_r - z_l}.$$

Thus the total velocity induced at z_r is

$$\overline{w}(z_r) = -a \, \mathrm{Sign}(\mathrm{Im}(z_r)) + \frac{a}{i\pi} \log \frac{z_r - \ell}{z_r + \ell} + \frac{1}{2i\pi} \frac{2a\ell}{z_r - z_l}, \tag{3}$$

which we can rewrite in terms of $\tan \alpha = h/\ell$

$$w(\alpha) = a \left(\mathrm{Sign}(\alpha) - \frac{1}{i\pi} \log \frac{i \tan \alpha}{2 + i \tan(\alpha)} - \frac{1}{2i\pi(1 + i \tan(\alpha))} \right) = aW(\alpha). \tag{4}$$

The symmetric self-similar solution is found at angle α_{ss} such that the velocity is aligned with Oz_r. Figure 2 shows that there is one single such angle $\alpha_{ss} \approx 26.7$. This is greater than the value of 18° obtained by [21].

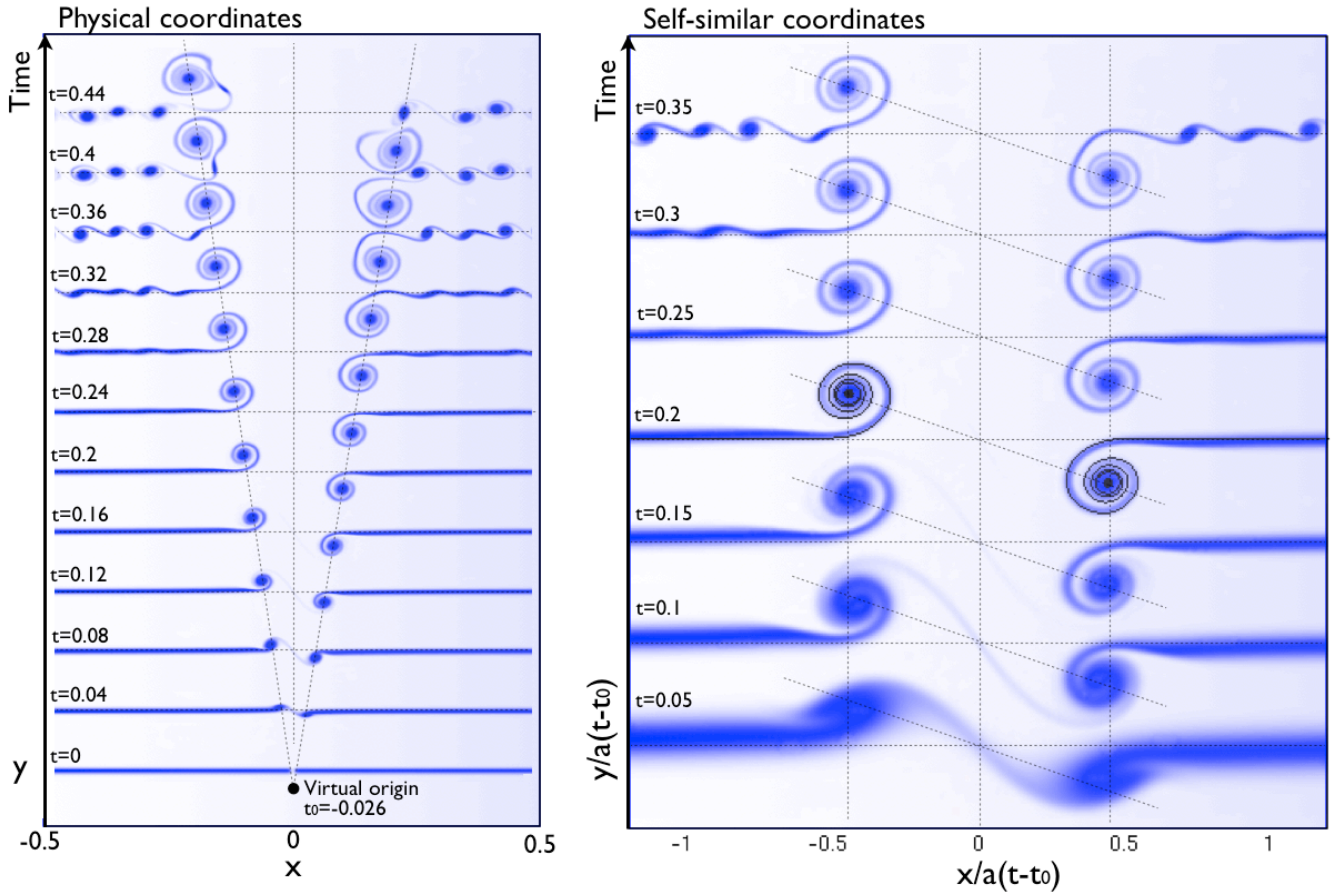

FIG. 3: Numerical simulation of the Euler equations in a horizontally periodic domain for a shear layer initially perturbed at its center. a) in physical coordinates and b) in self-similar coordinates. We dram as well the self-similar solutions digitized from [21] as a black line for time $t = 0.2$.

We consider now the velocity of the vortex. Supposing from initial time the vortex is located at this self-similar angle. Its induced velocity is $w(\alpha_{ss})$. The vortex position evolves according to

$$\dot{\ell} = |w(\alpha_{ss})| \cos \alpha_{ss} = a|W_{ss}| \cos \alpha_{ss},$$

which integrates into

$$\ell(t) = |W_{ss}| \cos \alpha_{ss} t.$$

To compare with Pullin's numerical simulation we express this in the self similar reference frame

$$\xi_{ss} = \frac{\ell}{at} = |W_{ss}| \cos \alpha_{ss} = 0.64, \quad \eta_{ss} = \frac{h}{at} = \xi \tan \alpha_{ss} = 0.32.$$

This gives an amplitude prefactor for the velocity of $V = 0.72$. This is greater than Pullin's computed value of 0.5. This means that the point vortex model overpredicts the rate of growth of the self-similar structure.

This data is shown in figure 2 where we draw in self-similar coordinates the self-similar solution digitized from [21] and the location (ξ_{ss}, η_{ss}) of our point vortex using a black dot. We show as well the velocity field induced by the untouched vortex sheet and the point vortex from (3).

A. Numerical solution of the Euler equations

Kaden's self-similar solution is well-known in relation to the wing-tip vortex of high aspect-ratio wings, but Pullin's self-similar solution is less known, so we need to demonstrate its relevance to shear layers of finite thickness. We can

find related numerical simulations in [10] for two-phase flows, in [17] for the application to ocean gravity waves and in [11] for the application to the atomization of a liquid jet. In the present paper we take the opportunity to compare directly with the evolution to the solution digitized from [21].

For the numerical solution, we use the open-source software *Gerris Flow Solver*, see [18]. The spatial discretization uses an octree adaptive mesh procedure and finite volumes. We use a streamfunction-vorticity formulation to solve the nonlinear evolution of the Euler equations. This formulation is well adapted to our flow with simple boundary conditions, and it allows to adapt the mesh refinement directly on the quantity of interest: the vorticity.

The computational domain is a unit square, periodic in the horizontal direction, and with symmetry boundary conditions at top and bottom. The flow is initiated as a sheet of vorticity of small thickness δ, with a local vorticity defect at the center of the domain

$$\omega(t=0) = -\frac{2}{\delta\sqrt{\pi}} e^{-(y/\delta)^2}(1 - e^{-(x/\delta)^2}).$$

This vortex sheet corresponds to an error function velocity profile of thickness 2δ with a velocity jump of 2 across the sheet, thus a value of the sheet strength parameter of $a = 1$. The velocity is -1 above the sheet and $+1$ below. This initial condition is akin to two semi-infinite vortex sheet next to each-other. The local defect of vorticity at the center will initiate the roll-up.

The mesh is adapted to the computational error based on vorticity, with a smallest grid size of $1/2^{10}$, thus the initial shear layer is resolved by 10 cells. The flow structure of interest rapidly grows in size, thus the relative resolution increases monotonously with time. This level of resolution would amount to about one million grid cells on an equivalent cartesian grid.

Gerris is a open-source software that can be easily downloaded and installed on linux distributions. The computation shown in this paper is exposed as a example for the use of streamfunction-vorticity formulation in Gerris. You may thus easily reproduce these simulation results using the parameter file available at [9]. The computational time is about 10 minutes on a standard single processor desktop computer.

The results are displayed in figure 3. We show the evolution in time of the vorticity field as a spatio-temporal diagram for selected times. On the left panel, we see the evolution in the physical coordinates. The color map shows a negative vorticity. We see initially the flat mixing layer, with a local defect at the center. At $(x = 0, y = 0)$ vorticity is zero, which can be thought as a positive vortex canceling locally the vorticity of the mixing layer. From this localized perturbation, the two semi-infinite layers roll-up on either sides. We see that the shape of the vorticity structure grows algebraically in time, according to the scaling from dimensional analysis. This shows that the mixing layer thickness δ has indeed a negligible effect on the dynamics of this impulse response flow, and thus the only physically relevant length scale is the velocity jump times t. Two straight lines drawn through the center of the spirals intersect at time $t_0 = -0.026$. This is not at initial time but slightly before, this is the virtual origin of the self-similar flow evolution. Indeed, initially the size of the flow structure is comparable to δ, and it is only after a short initial transient that the self-similar solution arises.

At $t = 0.28$, we start to see the Kelvin-Helmholtz instability of the straight mixing layer away from the central flow structure. This is the natural Kelvin–Helmholtz instability, initially excited probably from the long-range effect of the central structure, since a simulation run without the central vorticity defect (pure mixing layer) show that the mixing layer remains straight until at least $t = 0.35$ (not displayed here). It is encouraging to see that even though the mixing layer has destabilized into vortices along the complete width of the computational domain for $t > 0.36$, the algebraic growth of the central structure is still observed.

In the right panel of the figure, we show the evolution of the same simulation in the self-similar coordinates $x/(at), y/(at)$. In these coordinates, the self-similar solution should be a steady state of the evolution of the central structure. We see an initial transient from the perturbed mixing layer until time t of about 0.1, and then indeed the vorticity structure remains remarkably steady. For the last time shown, at $t = 0.35$, we see here again that despite the roll-up of the mixing layer, the spiral shape of the self-similar structure remains steady. At time $t = 0.2$ we have drawn the self-similar solution digitized from [21] upon the vorticity map. The agreement is remarkable. We may insist here on the fact that we are comparing two objects with very different origins: the colormap shows a snapshot from the time evolution of the Euler equation, with a thick mixing layer with a defect as initial condition; the solid black line is the steady solution of a nonlinear integro-differential equation for two semi-infinite sheets of velocity discontinuity transformed into similarity coordinates.

We take this figure has a confirmation of the relevance of Pullin's self-similar solution to the nonlinear impulse response of the Kelvin–Helmholtz instability. This direct numerical simulation recasts Pullin's solution into the context of intermediate asymptotics, as discussed in [2]. Self-similar solution of type I can be predicted based on dimensional analysis. Here indeed, if the mixing layer thickness is small compared to the characteristic size of the initial condition (δ), then the only length-scale of the evolution problem is $t\Delta U$. There is also a time scale introduced by the choice of an initial condition: the time it take for the specific initial condition to grow into the two-spiral

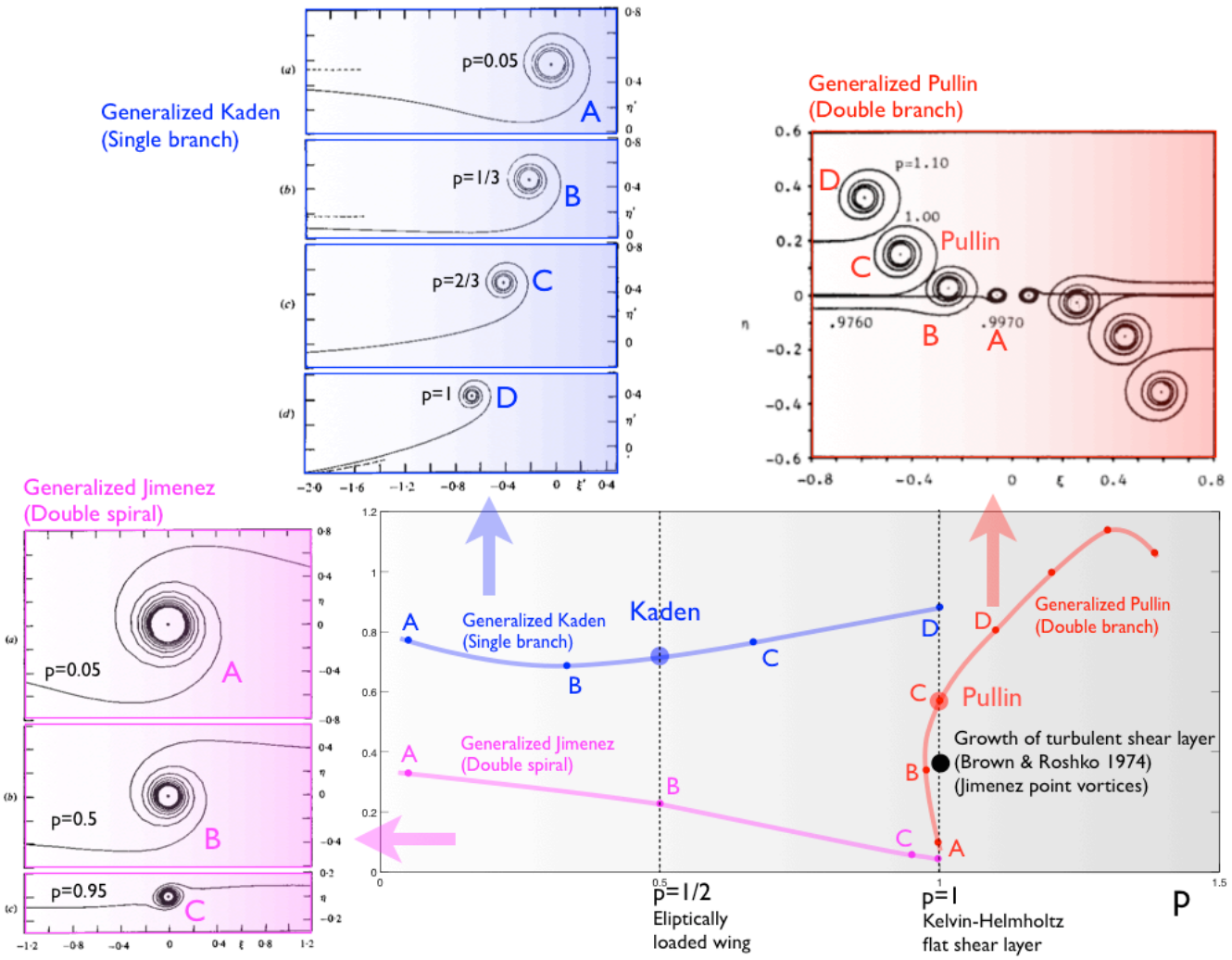

FIG. 4: Overview on the self-similar solutions of infinite shear layers. a) For three types of self-similar solutions, variation of the solution size as we vary the similarity exponent p. See text for the definition of the solution's size. Data is digitized from [20], [22] and [21]. We show as well the spatial growth rate of the turbulent mixing layer of [4] as cited in [12].

structure; this is the duration of the initial transient. Also, if the amplitude of other perturbations along the mixing layer is very small, it takes a long time for the associated vortices to appear, this is the destruction time scale. The self-similar solution has thus a range of existence in between the small time scale of the initial transient and the large time scale of the Kelvin–Helmholtz instability from noise; it thus appears as an intermediate asymptotic solution.

V. OVERVIEW OF SELF-SIMILAR SOLUTIONS FOR INFINITE VORTEX SHEETS

In this paper, we have focused on two particular cases of self-similar solutions for infinite vortex sheets: Kaden and Pullin. We may now consider the general context of vortex sheet with intensity varying according to a power law initial distribution

$$z_0(\Gamma) = (\Gamma/2a)^{1/p},$$

with exponent p. Kaden's solution is a one-branch structure for the similarity exponent $p = 1/2$, whereas Pullin's solution is a two-branch structure for the similarity exponent $p = 1$. [20–22] have generalized these self-similar solutions for a range of values of p. The particular value $p = 1/2$ is akin to the vorticity distribution near the tip in the wake of an elliptically loaded wing, so other kinds of loading are related to other values of p. Also for the vortex sheet, values of p different from unity may be though of as the mixing layer in the trail of a wing of incidence

varying along its span. In the following we will denote by *generalized Kaden* and *generalized Pullin* the continuation of Kaden's and Pullin's' solutions for other values of p.

We show in 4 a diagram for the size of the different similarity solutions as p is varied. The size S is defined as the distance from origo to the central vortex, digitized from [20–22]. The size of the generalized Kaden solution varies only slightly as p goes from 0.05 and tends to 1. For $p > 1.384$, Pullin's generalized solution does not have spirals, see [21], it is a single curved vortex sheet passing through origo. Below this critical value, the double-branch solution appears, and decreases progressively in size as p is lowered towards unity. Below $p = 1$, we see a peculiar behavior: a turning point, passed which we can follow the two-branch solution by increasing again p towards unity. This turning point means that for a given value of p in a small range below 1, there exist two independent two-branch solutions: a large one and a small one. Note that for $p = 1$, the infinite straight vortex sheet is as well a self-similar solution, a stationary one, with size $S = 0$ in this diagram.

For $p < 1$, [22] has exhibited yet a third family of similarity solutions, consisting of a double spiral: two vortex sheets roll into each other. This flow solution is reminiscent of the work of [12] and [13]. The hope of these papers was to exhibit a single-vortex similarity solution to the nonlinear impulse response of the Kelvin-Helmholtz instability. According to dimensional analysis, this nonlinear growth should have been algebraic, and the growth of the spiral vortex could be a tentative model for the algebraic spatial spread of the turbulent mixing layer of [4]. Unfortunately, the similarity solution could be found only approximately, and so the flow evolution was instead simulated by using a point-vortex method. In fact, we can read in [20] that "The limit p tends to 1 corresponds to that discussed by [12, 13] who reported considerable difficulty in seeking a solution to [the similarity equation]. Thus our results indicate that the unique spiral-type solution sought by Jimenez as a model for plane shear layer instability, does not exist." Nevertheless, in reminiscence of Jimenez's seminal work we may coin the double spiral solution at $p < 1$ the *generalized Jimenez* similarity solution.

In our model of Pullin's double spiral, we have chosen to locate the point vortex right above the edge of the vortex sheet. In fact we could free this constraint by locating the vortex at position $z = \beta\ell + ih$ where β is a free parameter which was set to 1 in §IV. Interestingly, when β is small, the self-similar solution we have described loses stability and a new steady state appear at $z = 0$, a situation reminiscent of Jimenez's solution.

For this similarity configuration, the central vortex is by symmetry located at origo, so we define its size as the maximum distance between the horizontal axis and the vortex sheet. Figure 4 shows that this family is much smaller than Kaden's and Pullin's, and that its size decays near zero when p approaches 1. The fact that the solution could not be continuated to $p = 1$ is a probable sign for a bifurcation. The double spiral becomes increasingly small in size towards $p = 1$, which would lead us to believe in the connection of this branch to the straight vortex sheet solution at size 0 and $p = 1$. This seems to be contradicted by the tendency of the curve in figure 4, but this is a possible artifact of an insufficient numerical resolution in [22].

The focus of Jimenez's work was the "visual growth" of the turbulent mixing layer behind the flat splitter plate of [4]. The spatial growth can be made into an analogy of a temporal growth by considering the mean advection velocity. The turbulent algebraic growth rate is thus about 0.38, see [12]. This situation pertains to an initial vortex sheet of constant intensity, thus $p = 1$. We have drawn this value on the diagram. Jimenez obtained a comparable growth rate in his numerical simulation of the impulse response of the Kelvin–Helmholtz instability. We see that this value is far from the continuation to $p = 1$ of the double-spiral solution, but that on the other hand it is not so far from the growth rate of Pullin's double branch solution.

VI. CONCLUSION

This paper belongs to a long filiation of research, starting with Helmholtz's idealization of a vortex sheet. The main aim is to describe how vortex sheets evolve under finite amplitude disturbances, combining parts that are in the process of being rolled-up into localized vortices, and parts that are still approximately straight. The behavior inside of the spiral core is known from the similarity solutions of [1, 14, 15, 19], and the remaining question is how to connect the infinitely wound spiral core to the large scale shape of the evolving vortex sheet. Pullin offered a major contribution by developing a numerical procedure to solve the Birkhoff-rott equations. He thus was in command of a quantitative tool to describe the process of sheet-spiral interaction. Also, he generalized Kaden's wing-tip vortex solution by considering vortex sheets with alternative distributions of intensity, and found two other similarity families, the double-branch spiral and the double-spiral. We have compared Pullin's solution to numerical marching of the Euler equation for an initial value problem and found a remarkable agreement. This is a further confirmation of the relevance of families of similarity solutions.

Pullin has developed an accurate numerical model, but what was obtained in precision was lost in complexity. The two final numeric values of the similarity angle and spiral velocity are obtained at the expense of a long process of mathematical and numerical manipulations. In the present paper, the aim was to contribute in the opposite range

of the modeling effort: provide the simplest possible model. Replacing the infinitely wound spiral by a point vortex and a straight sheet is a two-degrees of freedom model: $\ell + ih$ the position in complex plane of the point vortex. The model should be as simple as possible, but not simpler: would we remove one more degree of freedom, we lose the phenomenon of similarity altogether. This model has a self similar solution, it gives reasonable values of the angle and velocity and the steps of derivation are elementary. Moreover, the model shows that the self-similar solution is indeed stable with a large basin of attraction.

An overview of the similarity families was given in figure 4 by gathering data from the literature. The continuation structure of the three families when the similarity exponent is varied seems not completely understood. Does the double-spiral bifurcate into the flat shear layer when p tends to 1? Does the double-branch as well bifurcate to the flat shear layer? In Pullin's paper, the double-branch family experiences a turning point below $p = 1$. Is this related to a global loss of stability of the self-similar solution? Can we trust the structure of the bifurcation diagram from Pullin's simulation? Pullin concludes himself in [21]: "Finally, we note that to date no search has been made for bifurcation off the solution curves [...], which may extend the single-spiral solutions to $p < 0.9666$. Likewise we have not attempted to extend the double-spiral solutions to $p > 1$. This may lead to further rich structure for the unbounded similarity flows containing vortex sheets."

The precise mapping of this bifurcation diagram may be of fundamental interest. For the study of transition to turbulence in pipe flows, the absence of a critical Reynolds number for linear instability has led to a strong interest in the behaviour and stability of nonlinear traveling waves. These waves are special nonlinear solutions to the Navier–Stokes equations, periodic in time and in space. These flow solutions play the role of dynamic saddle points for the evolution of finite amplitude perturbation on the parabolic base flow, and thus play a strong role in the organization of the transition process and turbulent dynamics, see [6]. We may speculate as a conclusion to the present paper that the several families of self-similar sheet-spiral evolution may play as well a globally structuring role in the nonlinear dynamics of mixing layers.

[1] Alexander, R. C. 1971 Family of similarity flows with vortex sheets. *Phys. Fluids* **14** (231).
[2] Barenblatt, G. I. 2006 *Scaling*. Cambridge University Press, Cambridge.
[3] Batchelor, G. K. 1967 *An introduction to fluid dynamics*. Cambridge university press, New York.
[4] Brown, GL & Roshko, A 1974 Density effects and large structure in turbulent mixing layers. *J. Fluid Mech.* **64** (JUL24), 775.
[5] Devenport, W. J., Rife, M. C., Miapis, S. I. & Follin, G. J. 1996 The structure and development of a wing-tip vortex. *J. Fluid Mech.* **312**, 67–106.
[6] Eckhardt, B., Schneider, T. M., Hof, B. & Westerweel, J. 2007 Turbulence transition in pipe flow. *Annu. Rev. Fluid Mech.* **39**, 447–468.
[7] Eggers, Jens & Fontelos, Marco 2009 The role of nonlinearity in singularities of partial differential equations. *Nonlinearity* **22**.
[8] Helmholtz, Hermann 1868 On discontinuous movements of fluids. *Phil. Mag. series 4* **36**, 337–346.
[9] Hoepffner, Jérôme 2013 Vorticity-streamfunction example of the gerris flow solver.
[10] Hoepffner, Jérôme, Blumenthal, Ralf & Zaleski, Stéphane 2011 Self-similar wave produced by local perturbation of the kelvin-helmholtz shear-layer instability. *Physical Review Letters* **106** (10).
[11] Jerome, J. John Soundar, Marty, Sylvain, Matas, Jean-Philippe, Zaleski, Stéphane & Hoepffner, Jérôme 2013 Vortices catapult droplets in atomization. *Phys. Fluids* **25** (112109).
[12] Jimenez, J. 1978 Numerical simulation of mixing layer vortices. In *Structure and Mechanisms of Turbulence I* (ed. H. Fiedler), *Lecture Notes in Physics*, vol. 75, pp. 147–161. Springer Berlin / Heidelberg.
[13] Jimenez, J. 1980 On the visual growth of a turbulent mixing layer. *J. Fluid Mech.* **96**, 447–460.
[14] Kaden, H. 1931 Aufwicklung einer unstabilen unstetigkeits flache. *Ing. Archiv.* **2** (140).
[15] Kambe, T. 1989 Spiral vortex solution of Birkhoff-Rott equation. *Physica D* **37**, 463–473.
[16] Moore, D. W. 1975 The rolling up of a semi infinite vortex sheet. *Proc. Roy. Soc. A* **345**, 417–430.
[17] Orazzo, Annagrazia & Hoepffner, Jérôme 2012 The evolution of a localized nonlinear wave of the kelvin–helmholtz instability with gravity. *Phys. Fluids* **24** (112106).
[18] Popinet, Stéphane 2009 An accurate adaptive solver for surface-tension-driven interfacial flows. *J. Comp. Phys.* **228**, 5838–5866.
[19] Prandtl, L. 1961 Uber die entstehung von wirbeln in der idealen flussigkeit (1922). In *Gessamette abhandlungen*, , vol. 2, pp. 697–713. Springer, Berlin.
[20] Pullin, D. I. 1978 The large scale structure of unsteady self-similar rolled-up vortex sheets. *J. Fluid Mech.* **88** (3), 401–430.
[21] Pullin, D. I. 1989 On similarity flows containing two-branched vortex sheets. In *Mathematical Aspects of Vortex Dynamics* (ed. R. E. Caflisch), pp. 97–106. Society for Industrial and Applied Mathematics, Philadelphia.
[22] Pullin, D. I. & Phillips, W. R. C. 1981 On a generalisation of kaden's problem. *J. Fluid Mech.* **104**, 45–53.
[23] Saffman, P. G. 1992 *Vortex dynamics*. Cambridge University Press.

[24] Thomas, P.J. & Auerbach, D. 1994 The observation of the simultaneous development of a long- and a short-wave instability mode on a vortex pair. *J. Fluid Mech.* **265**, 298–302.